Coherent control over Liouville-space pathways interference in transient four-wave mixing spectroscopy

Pshenichnikov, M.S; de Boeij, W.P.; Wiersma, D. A.

Link to publication in University of Groningen/UMCG research database

Coherent Control over Liouville-Space Pathways Interference in Transient Four-Wave Mixing Spectroscopy

Maxim S. Pshenichnikov, Wim P. de Boeij, and Douwe A. Wiersma

Ultrafast Laser & Spectroscopy Laboratory, Department of Chemistry, Materials Science Centre, University of Groningen, Nijenborgh 4, 9747 AG Groningen, The Netherlands

(Received 11 March 1996)

A novel interference effect in transient four-wave mixing is demonstrated. The phenomenon is based on phase-controlled Liouville-space pathways interference and observed in the heterodyne-detected stimulated photon echo. Changing the phase difference between the first two excitation pulses from $\pi/2$ to 0 leads from no signal to maximum echo signal. A Brownian oscillator dynamical model is successfully used to analyze the effect and simulate the experimental data. The relation between this time-domain interference effect and dephasing-induced resonance in four-wave mixing spectroscopy is elaborated. [S0031-9007(96)00451-6]

One of the most remarkable phenomena in cw four-wave mixing spectroscopy concerns the effect of dephasing on an initially unpopulated excited-state resonance [1–3]. In this experiment the coherent Raman signal is monitored as a function of frequency difference between the exciting light fields. When the frequency difference equals an excited-state splitting, one might expect, intuitively, the Raman signal to reflect the combined resonance. However, this turns out not to be the case, unless the system is perturbed by collisions which induce dephasing on the optical transitions. The effect, denoted as PIER-4 (pressure-induced extra resonance in four-wave mixing), was first reported by Bloembergen and co-workers on sodium in the gas phase [1] and later also demonstrated for condensed phase molecular systems by Hochstrasser and co-workers [2].

Dephasing-induced resonances can be grasped most easily in terms of interference between different Liouville-space pathways which describe the generation of the relevant third-order optical polarization responsible for the four-wave mixing signal. It can be shown that, in the absence of collisions, the different excitation pathways interfere destructively with one another and that no net polarization is generated [1]. When, with increase in pressure or temperature, dephasing effects become important, the Liouville-space pathways are no longer equivalent, and, as a result, a finite nonlinear optical polarization is generated.

Interestingly enough, when this coherent Raman experiment is performed in the time domain using two time-coincident short optical pulses of different color—short compared to the inverse transition linewidth—the excited state resonance is always found, irrespective of whether the system experiences pure dephasing or not [4,5]. The essential difference with the cw case is that for pulsed excitation they system has no time to evolve appreciably within the pulse duration [6]. Relaxation towards the steady state is thus essential for destructive interference effects in cw

coherent Raman spectroscopy. In view of this fact it seems unlikely that dephasing-induced interference effects play a role in time-domain four-wave mixing spectroscopy.

In this Letter we report on the observation of a novel dephasing-induced interference effect in phase-locked stimulated photon echo. The phenomenon is demonstrated on a dye solution at room temperature. We show that in such a non-Markovian dynamical system, Liouville-pathway interference effects are important in generating the nonlinear polarization and that it is possible to exercise phase control over this effect.

The pulse sequence used [Fig. 1(a)] is that of a stimulated photon echo [7]. In such an experiment two ultra-
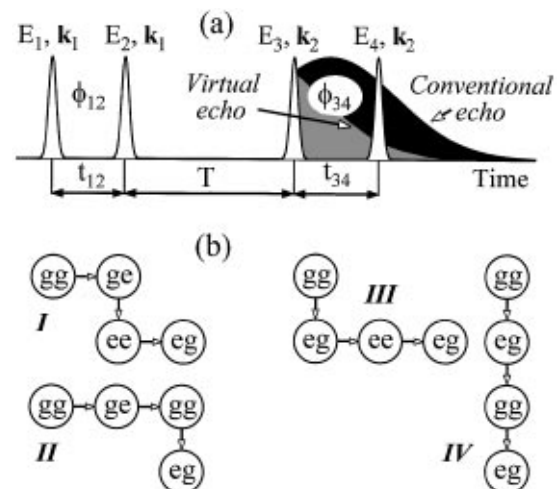
FIG. 1. Pulse sequence for heterodyne detection of stimulated photon echo (a) and the basic Liouville pathways used for a perturbative description of the third-order polarization $P^{(3)}$ with wave vector $\mathbf{k}_1 - \mathbf{k}_1 + \mathbf{k}_2$ in a two-level system with ground $|g\rangle$ and excited $|e\rangle$ states (b). All pulses are supposed to be well separated in time. The symbols in open circles (*gg*, *ge*, etc.) denote the density matrix elements which characterize the system evolution after each subsequent perturbation (arrows). The diagrams I and II describe the conventional echo while III and IV lead to virtual echoes.

short pulses E_1 and E_2 excite the system, which is then probed by a third pulse E_3 at the so-called waiting time T. The generated third-order nonlinear polarization $P^{(3)}$ subsequently emits a transient coherent signal, photon echo, in the phase-matched direction $\mathbf{k}_2$. Crucial to the interference effect is the fact that the wave vectors of the fields E_1 and E_2 are identical.

The nonlinear polarization, induced by the excitation pulses, can be described using the four basic Liouville-space diagrams [8] depicted in Fig. 1(b) [9,10]. In a similar fashion to the pressure-induced resonance case [6], interference occurs between two pathways that drive the system from the ground state $|g\rangle\langle g|$ to the excited state $|e\rangle\langle e|$ via a coherent superposition $|g\rangle\langle e|$ [diagram I in Fig. 1(b)] or $|e\rangle\langle g|$ [diagram III in Fig. 1(b)]. Since photon echo is a degenerate four-wave mixing effect, the evolution of the system in the ground state needs to be taken into account as well [diagrams II and IV in Fig. 1(b)].

In case of an inhomogeneously broadened system, the so-called rephasing diagrams I and II generate a polarization which peaks after the third excitation pulse [Fig. 1(a)]. This signal is the well-known conventional stimulated photon echo [11]. In the Bloch model, for instance, the temporal profile of the photon echo signal is proportional to $\exp[-(t + t_{12})/T_2 - (t - t_{12})^2/2T_2'^2]$, where T_2 is the phase relaxation time and T_2' is the inhomogeneous dephasing time [7]. The nonrephasing diagrams III and IV lead to the so-called *virtual echo* [12]. Its temporal profile is given by $\exp[-(t + t_{12})/T_2 - (t + t_{12})^2/2T_2'^2]$ [7]. Mathematically, the virtual echo has the same shape as the conventional one, but its maximum occurs at $t = -t_{12} - T_2'/T_2$, i.e., *before* the last excitation pulse. Because of causality, only the tail ($t \geq 0$) of the virtual echo following the third excitation pulse can be measured, as depicted in Fig. 1(a). Because the conventional and virtual echoes are emitted in the same direction, $\mathbf{k}_2$, they can, in principle, interfere. By heterodyning the resulting electric field with a fourth pulse, E_4, both the temporal shape and the phase of the resulting polarization can be determined. The described pulse sequence [Fig. 1(a)], known as heterodyne-detected stimulated photon echo (HSPE), was first proposed by Cho *et al.* as a probe for solvation dynamics [9]. However, in their analysis the virtual echo contribution to the signal

was ignored. This contribution, however, turns out to be essential for the interference effect in phase-locked photon echo.

To calculate the HSPE signal, which is proportional to all applied optical fields, $S \propto \text{Re}(P^{(3)} E_4^*)$, we need a dynamical model. For this we take the Brownian oscillator (BO) model which has been described extensively in the literature [8]; we therefore just mention a few points relevant to the experiment. In the BO model, the interaction of a two-level system with the heat bath is mediated by a so-called Brownian oscillator, whose correlation function $M(t)$ characterizes the dynamical properties of the system-bath interaction. For instance, for a homogeneously broadened system. $M(t) = \delta(t)$, while for an inhomogeneously broadened system $M(t) = 1$. Next to $M(t)$ there are two other important parameters needed to calculate the polarization. The first one is Δ, which is a measure of the coupling strength between the optically active chromophore and its environment (bath). The second important quantity is λ, the reorganization or solvation energy. In the so-called high temperature limit, Δ and λ are connected by the relation $\lambda \approx \Delta^2 \hbar/2k_B T_k$ [8]. This limit is often applied in a first-order theoretical description of solution optical dynamics. So, once Δ, λ, and $M(t)$ are known, the induced polarization in any linear or nonlinear experiment can be calculated. Here we do not assume a particular form of the correlation function, but, for the sake of mathematical simplicity, we take the correlation function not to be short compared to the time scales of t_{12} and t_{34} (but no T). We also assume the excitation pulses to be short compared to the inverse width of the chromophore spectrum (impulsive excitation). With these assumptions, the HSPE signals can be readily calculated. The resulting expressions for the phase difference ϕ_{12} and ϕ_{34} being 0 and $\pi/2$ are given in Table I. Despite the rather severe assumptions made, we will see that this theoretical framework captures all important features of the experiment.

Figure 2 shows the schematics of the setup used for the exploration of the interference effect in HSPE. The 13 fs laser pulses, derived from a home-built cavity-dumped (CD) Ti:sapphire laser [13], are split and fed into two identical Mach-Zehnder interferometers MZI-1 and MZI-2. Since phase fluctuations should be minimized, each interferometer is actively stabilized by a feedback loop [14]. Briefly, after the interferometers each pulse pair is dispersed through a monochromator. Because of the interference between two stretched pulses, the resulting power spectrum becomes modulated by $\cos(\omega\tau + \phi)$, where τ is the time separation between the pulses and ϕ is their phase difference. The monochromator output is used as a feedback signal that drives a piezotransducer in one of the interferometer arms to compensate for any phase drift. In this manner the delay between the copropagating pulses is set within ± 10 attosecond accuracy. This arrangement also allows for locking the phase differences

TABLE I. The expressions for the HSPE signals for different phase settings in the impulsive approximation. Here, $S_E = \exp[-\Delta^2/2(t_{12}^2 + t_{34}^2 - 2M(T)t_{12}t_{34})]$ is the conventional echo, $S_{VE} = \exp[-\Delta^2/2(t_{12}^2 + t_{34}^2 + 2M(T)t_{12}t_{34})]$ the virtual echo, $\alpha = \cos^2\{[\lambda t_{34}(1 - M(T))]\}$ and $\beta = 1/2 \sin\{2\lambda t_{34}[1 - M(T)]\}$ the phase factors due to the bath relaxation, Δ the coupling strength of the system-bath interaction, and λ the bath reorganization energy.

Phases	$\phi_{12} = 0$	$\phi_{12} = \pi/2$
$\phi_{34} = 0$	$\alpha(S_E + S_{VE})$	$\beta(S_E - S_{VE})$
$\phi_{34} = \pi/2$	$-\beta(S_E + S_{VE})$	$\alpha(S_E - S_{VE})$

ϕ_{12} and ϕ_{34} at any value during a scan of the delays t_{12} or t_{34} [10]. The echo signal is generated by focusing the two beams containing the pulse pairs E_1-E_2 and E_3-E_4 into a 100 μm jet of a dye solution at room temperature. As solvent we use ethylene glycol, while the dye molecule is $3,3'$-diethylthiatricarbocyanine iodide (DTTCI). This dye molecule is chosen because its absorption spectrum matches nicely that of the laser. The HSPE signal is detected by a silicon photodiode and processed by a lock-in amplifier.

Figure 3 displays phase-locked HSPE signals for four different phases and at different waiting times. In this experiment, the delay t_{34} between pulses E_3 and E_4 is scanned, while the delay t_{12} between pulses E_1 and E_2 is fixed at a certain value. It should be noted that similar signals were observed at different delays t_{12}. Inspection of Table I shows that the detected HSPE signal is the sum of two different contributions: the conventional echo and virtual echoes (both heterodyne detected), which are generated via different excitation pathways. If $\phi_{12} = 0$, these contributions add constructively (Fig. 3, left panels), and an enhanced echo signal results. When $\phi_{12} = \pi/2$, a phase shift of π occurs between the conventional and virtual echo signals. The resulting destructive interference leads to suppression of the echo (Fig. 3, right panels). The echo signal completely vanishes at $T = 200$ ps. By this time, the real and virtual echoes have merged in time, which happens when the system has lost all phase memory [10]. Two "echoes" have become indistinguishable, and complete destructive interference occurs between equal amplitude but oppositely phased Liouville pathways. In contrast, for shorter waiting times, the interference is incomplete because the real and virtual echo fields peak at different times. Waiting-time dependent HSPE signals for $\phi_{12} = \pi/2$ thus clearly exhibit the transition from a partly inhomogeneously to a homogeneously broadened system with increasing time. The observed narrowing of the signals with time is caused by the same effect. There is another aspect of the HSPE signals that deserves attention. As Fig. 3 shows, just by changing the phase difference between the first two pulses by $\pi/2$, one switches from the case of full constructive to complete-destructive interference. This presents a prime example of coherent control of a nonlinear optical polarization.
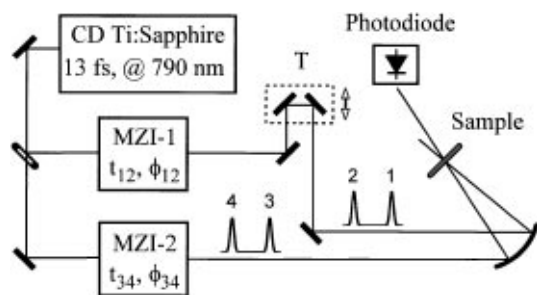
The solid lines in Fig. 3 are the fits to the echo signals calculated on the basis of the expression given in Table I. To perform these calculations we need Δ, which was estimated from the width of the absorption spectrum to be about 270 cm^{-1}. The reorganization parameter λ then equals 175 cm^{-1} when we assume the high temperature limit of the BO model to hold. The finite pulse duration was taken into account by convolution of the computed signals with an apparatus response function. At this point, the only unknowns are the value of the correlation function $M(T)$ at the selected waiting times and an overall signal amplitude (the same for all 16 curves). Considering the approximations made, the correspondence between theory and experiment is remarkable and leaves no doubt about the basic gasp of this interference effect.

Table I shows that the HSPE signals for the combination of phase factors ($\phi_{12} = \pi/2$, $\phi_{34} = 0$) and ($\phi_{12} = 0$, $\phi_{34} = \pi/2$) exist only when the bath reorganization energy λ is finite or, to put it differently, that the excited chromophore induces a reorganization of the solva-
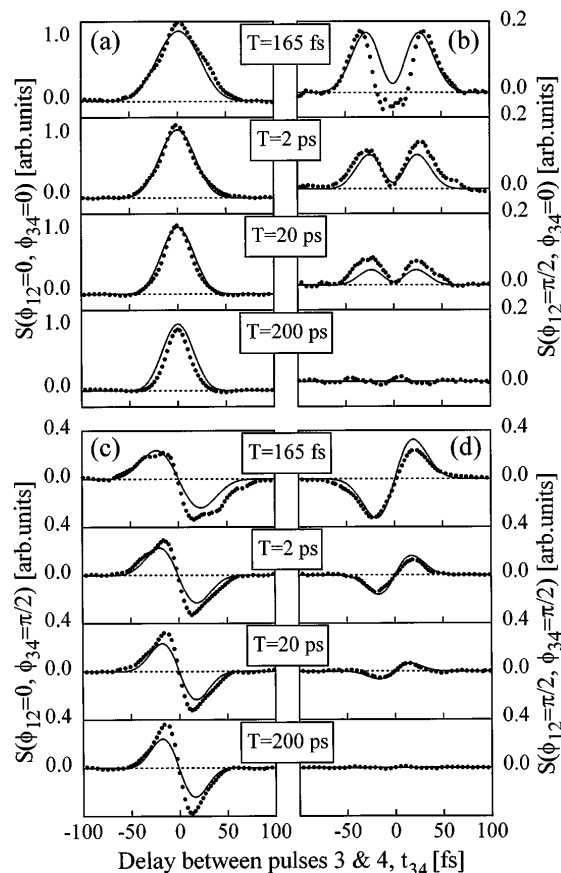

FIG. 3. Heterodyne-detected stimulated photon echo for phase settings $\phi_{12} = 0$, $\phi_{34} = 0$ (a), $\phi_{12} = \pi/2$, $\phi_{34} = 0$ (b), $\phi_{12} = 0$, $\phi_{34} = \pi/2$ (c), and $\phi_{12} = \pi/2$, $\phi_{34} = \pi/2$ (d). The delay between pulse E_1 and E_2 is 40 fs while the pulse energies are ~ 0.15 nJ. The numerical simulations shown as solid lines yielded the following values of the correlation function: $M(165 \text{ fs}) = 0.36$, $M(2 \text{ ps}) = 0.21$, $M(20 \text{ ps}) = 0.09$, and $M(200 \text{ ps}) = 0$.

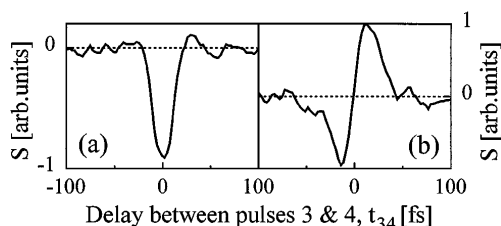FIG. 2. Schematics of the experimental setup.

FIG. 4. High-intensity heterodyne-detected stimulated photon echo signals at $T = 200$ ps. Phase settings are $\phi_{12} = \pi/2$, $\phi_{34} = 0$ (a) and $\phi_{12} = \pi/2$, $\phi_{34} = \pi/2$ (b). The delay between pulses E_1 and E_2 is 40 fs while the pulse energies are ~ 1 nJ.

tion shell [8]. It is pertinent to point out here that the fact that these signals are observed [Figs. 3(b) and 3(c)] is consistent with the BO model. Other often-used models to describe optical dynamics, such as the Bloch or a stochastic model [8,15], predict these signals to be nonexistent, in clear contradiction with experiment.

At higher laser intensities, fifth-order nonlinearity has to be taken into account. As an example, we display in Fig. 4 two HSPE signals which are nonexistent at lower intensities (Fig. 3). These echo signals can be shown to be generated through an intermediate population state during the time interval t_{12}. The interplay between third- and fifth-order nonlinearities will be addressed in more detail elsewhere [16]. Fifth-order effects have also been predicted in PIER-4 [17] but not reported yet.

In closing, we wish to address the question of how the interference effect in phase-locked echo is related to the phenomena of dephasing-induced resonance in four-wave mixing. Of course, both effects are manifestations of interference between different Liouville pathways. However, for the rest, the effects are quite different. In the dephasing-induced-resonance case the two excitation pathways are, in the absence of collisions, oppositely phased, and hence no net polarization is formed. It is only after collisions have randomly changed the phase between the excitation pathways that a coherent signals can be generated [1–3,6]. In phase-locked heterodyne-detected echo, dephasing (for instance, induced by collisions between chromophore and solvent molecules) plays quite a different role in the interference between excitation pathways. First, whether or not dephasing occurs, the effect of interference between the real and virtual echo signals is always there. Second, the phase between the interfering Liouville pathways is not determined by collisions but imposed on the system from the outside. In this case, dephasing drives the virtual and real echoes to merge in time, when the system has lost all phase memory. At that point, the pathways can be made to interfere completely destructively.

Summarizing, we have described a novel interference effect in phase-locked stimulated photon echo, which, as usual, relies on the interplay between different excitation pathways. Active control of the relative phases of the excitation pulses allows for switching between constructive and destructive interference. This technology is also of a special interest to coherent control experiments in chemistry, where Liouville-space pathway interference is an important option [18].

[1] N. Bloembergen, H. Lotem, and R. T. Lynch, Ind. J. Pure Appl. Phys. **16**, 151 (1978); Y. Prior *et al.,* Phys. Rev. Lett. **46**, 111 (1981); A. Bogdan, M. Downer, and N. Bloembergen, Phys. Rev. A **24**, 623 (1981).

[2] J. R. Andrews and R. M. Hochstrasser, Chem. Phys. Lett. **82**, 381 (1981); **83**, 427 (1981); J. R. Andrews *et al.,* Chem. Phys. **62**, 87 (1981).

[3] S. A. J. Druet *et al.,* Phys. Rev. A **18**, 1529 (1978); G. S. Agarwal and J. Cooper, Phys. Rev. A **26**, 2761 (1982); G. S. Agarwal and C. V. Kunasz, Phys. Rev. A **27**, 996 (1983); Y. Prior, I. Schek, and J. Jortner, Phys. Rev. A **31**, 3775 (1985).

[4] D. P. Weitekamp, K. Duppen, and D. A. Wiersma, Phys. Rev. A **27**, 3089 (1983).

[5] K. Duppen, D. P. Weitekamp, and D. A. Wiersma, in *Time-resolved Vibrational Spectroscopy,* edited by A. Laubereau and M. Stockburger (Springer-Verlag, Berlin, 1985), p. 112.

[6] S. Mukamel and R. F. Loring, J. Opt. Soc. Am. B **3**, 595 (1986).

[7] K. Duppen and D. A. Wiersma, J. Opt. Soc. Am. B **3**, 614 (1986).

[8] S. Mukamel, *Principles of Nonlinear Optical Spectroscopy* (Oxford University Press, New York, 1995).

[9] M. Cho *et al.,* J. Chem. Phys. **96**, 5618 (1992).

[10] W. P. de Boeij, M. S. Pshenichnikov, and D. A. Wiersma, Chem. Phys. Lett. **238**, 1 (1995).

[11] L. Allen and J. H. Eberly, *Optical Resonance and Two-Level Atoms* (New York, 1975).

[12] A. L. Bloom, Phys. Rev. **98**, 1105 (1955).

[13] M. S. Pshenichnikov, W. P. de Boeij, and D. A. Wiersma, Opt. Lett. **19**, 572 (1994).

[14] N. F. Scherer *et al.,* J. Chem. Phys. **93**, 856 (1990); **95**, 1487 (1991).

[15] E. T. J. Nibbering, D. A. Wiersma, and K. Duppen, Chem. Phys. **183**, 167 (1994).

[16] W. P. de Boeij, M. S. Pshenichnikov, and D. A. Wiersma (to be published).

[17] B. Dick and R. M. Hochstrasser, Chem. Phys. **75**, 133 (1983).

[18] D. J. Tanner and S. A. Rice, Adv. Chem. Phys. **70**, 441 (1988); P. Brumer and M. Shapiro, Acc. Chem. Res. **22**, 407 (1989); P. Brumer and M. Shapiro, Sci. Am. **272**, 34 (1995).